JOURNAL OF AIRCRAFT
Vol. 35, No. 5, September–October 1998

Influence of Model Complexity and Aeroelastic Constraints on Multidisciplinary Optimization of Wings

Jonathan A. Bishop*
U.S. Air Force Research Laboratory, Kirtland Air Force Base, New Mexico 87117-5776
Franklin E. Eastep†
University of Dayton, Dayton, Ohio 45469-0027
Alfred G. Striz‡
University of Oklahoma, Norman, Oklahoma 73019-0601
and
Vipperla B. Venkayya§
U.S. Air Force Research Laboratory, Wright–Patterson Air Force Base, Ohio 45433-7542

This investigation focuses on the performance of the Automated Structural Optimization System multidisciplinary optimization code in the structural weight optimized design of two finite element models of a low-aspect ratio fighter-type wing. Optimal designs for the wing with the structure represented by a coarse and a more complex finite element model are obtained with constraints imposed on strength, aileron reversal, and flutter using subsonic and supersonic aerodynamic theories. The results demonstrate the ability of ASTROS to effectively find local minima with weight as the objective function. The trends in the final weights illustrate the impact of changing design constraints on optimal design.

Introduction

AN aircraft structural designer must consider aeroelastic instabilities, i.e., flutter and divergence, in addition to strength and stiffness, e.g., aileron reversal, requirements in the development of a high-performance aircraft. In particular, he must design a structure such that the critical aeroelastic speed is at least 15% above the maximum operational flight speed while still ensuring satisfactory strength and stiffness at this speed. The critical aeroelastic speed is defined as the lowest of the flutter, divergence, or aileron reversal speeds. At the same time, the structural designer desires to adjust the structural sizes to minimize overall structural weight.

In recent years, structural optimization as needed and used by the aerospace industry has expanded in scope to include such additional disciplines as static and dynamic aeroelasticity, composite materials, aeroelastic tailoring, etc. One of the more promising existing multidisciplinary codes is the Automated Structural Optimization System (ASTROS).[1–3] In this computer code, static, dynamic, and frequency response finite element structural modules, subsonic and supersonic steady and unsteady aerodynamic modules, and an optimization module are combined and allow for either analysis or optimized design of given aircraft configurations. Interfering surface aerodynamics are incorporated to handle the aerodynamic modeling of combinations of wings, tails, canards, fuselages, and stores. Structures are represented by fully built-up finite element models, constructed from rod, membrane, shear, plate, and other elements. Static and dynamic aeroelastic capabilities include trim, lift effectiveness, control effectiveness, gust response, and flutter analysis. The optimization and aeroelasticity modules of this code were used here as a tool for the structural optimization of fully built-up finite element wing models in subsonic and supersonic flow with strength as well as static and dynamic aeroelastic constraints.

Background and Objectives

With the continuing increase in computing power, structural optimization is becoming a more likely tool for practical engineering problems. For stress and load-type constraints, both size and shape optimizations are useful design techniques. For aircraft component design, however, these techniques require detailed external load calculations that are not typically available until after overall geometry has been determined. Thus, automated optimization has not been applied widely to the macrolevel design of wing and other aircraft structures because of the unsuitability to optimization of accurate, large degree-of-freedom models. Reduced degree-of-freedom models could be used for some aspects of preliminary design provided they can approximate detailed structural and aeroelastic behavior with some accuracy.

The purpose of this investigation is to determine the effects of model complexity on the final optimized design of wings when aeroelastic constraints are imposed. Such results are useful for two reasons. First, Yurkovich[4] found that the final weight for a series of wings optimized for flutter and static load was largely independent of internal geometry, i.e., the number of ribs and spars, but was strongly a function of external variables such as chord and aspect ratio. The present effort will build on this result by analyzing and optimizing two wings with nearly identical external shapes but with different internal configurations.

Second, the present work will determine the sensitivities of more complex multi-constraint optimizations to slight differences in structural properties. Although the wings were chosen to have similar structural properties, their properties were not matched by optimization, and some differences still exist. Such

Presented, in part, as Paper 91-1100 at the AIAA/ASME/ASCE/AHS/ASC 32nd Structures, Structural Dynamics, and Materials Conference, Baltimore, MD, April 8–10, 1991; received June 16, 1996; revision received Feb. 28, 1998; accepted for publication March 10, 1998. This paper is declared a work of the U.S. Government and is not subject to copyright protection in the United States.

*Space Systems Project Engineer, AFRL/VSDV, 3550 Aberdeen Avenue, SE. E-mail: bishopj@plk.af.mil. Member AIAA.

†Professor, Department of Mechanical and Aerospace Engineering. Associate Fellow AIAA.

‡Associate Professor, School of Aerospace and Mechanical Engineering. Associate Fellow AIAA.

§Principal Scientist, AFRL/VAS, 2130 Eighth Street, Suite 1. Fellow AIAA.

structural differences will result in slight performance differences for the nominal wings because, for example, the structural behavior, which depends on the sizes of the structural members, influences the flutter behavior, i.e., the flutter speed and the flutter mode shapes, as asserted by Striz and Venkayya.[5] As the wing model is optimized, the thicknesses of the structural members are adjusted in each iteration, changing the normal modes and flutter behavior. The same essentially holds for such constraints as aileron effectiveness and strength. Thus, any differences in the nominal analysis may be compounded during optimization. Even minor deviations can be exaggerated in the results as pointed out by Striz and Venkayya.[6] By optimizing the two models, the present work will therefore determine whether these models of differing complexities have approximately the same optimal weights; thus, allowing the simpler model to be used for quick optimization in a complex design space.

Structural and Aerodynamic Modeling

The two low-aspect ratio wing structural models were selected to be representative of a fighter-type wing of idealized wing planform with an aileron located near the wingtip. The underlying structure of each wing was fully built up using finite elements. These models were optimized for minimum weight under strength as well as static and dynamic aeroelastic constraints. The first (Fig. 1) was a coarse model with 86 structural grid points. The complex second model (Fig. 2) had 550 structural grid points. The geometry and the dimensions of the wing model are given in Fig. 3, which shows the coarse structural model and the aerodynamic models used for flutter and steady aeroelastic analysis. The more complex model had identical exterior dimensions. The aerodynamic model used for steady aeroelastic analysis was similar to the flutter model, except that it extended to the aircraft centerline. The structure of each wing model are outlined next.

1) Coarse design low-aspect ratio wing (M = 0.85 and 1.2, sea level): Constraints = strength (von Mises), reversal, flutter. Input = shear panel thickness, 0.08 in. ribs, 0.075–0.03 in. (interior spars), and 0.135–0.05 in. (front and rear spars). Membrane thickness, 0.25–0.04 in. skins. Spar cap cross-sectional area, 1.0–0.5 in.^{2} (interior spars) and 1.75–0.88 in.^{2} (front and rear spars). Spar stiffener cross-sectional area, 0.05 in.^{2} (not designed). (All values decreasing from root to tip.) Material = $E = 1.0 \times 10^7$ lb/in.^{2}, $\nu = 0.33$, $\rho = 0.1$ lb/in.^{3} Allowable stresses: 60×10^3 lb/in.^{2} (tension and compression), 40×10^3 lb/in.^{2} (shear).

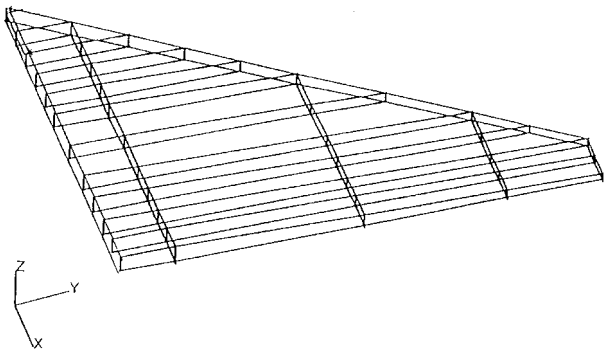

Fig. 1 Coarse structural model.

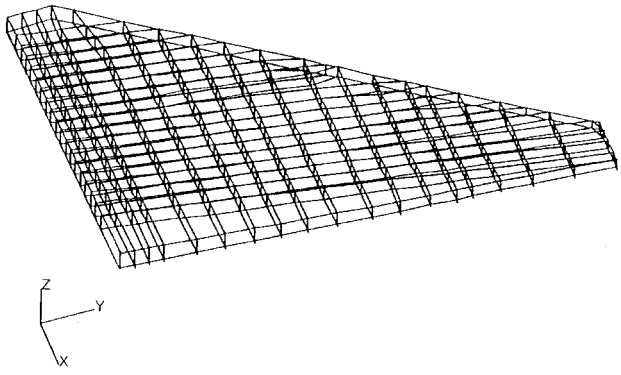

Fig. 2 Complex structural model.

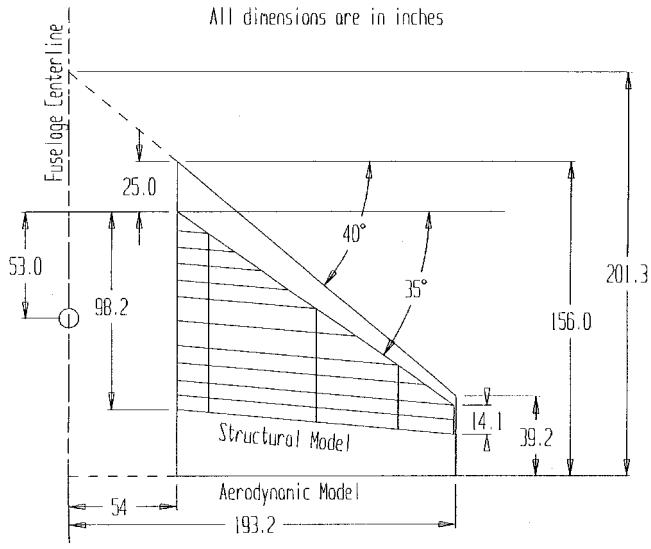

Fig. 3 Aerodynamic and structural model geometry and dimensions.

2) Complex design low-aspect ratio wing (M = 0.85 and 1.2, sea level): Constraints = strength (von Mises), reversal, flutter. Input = shear panel thickness, 0.015 in. ribs, 0.062–0.005 in. (interior spars), and 0.154–0.0605 in. (front and rear spars). Membrane thickness, 0.25–0.046 in skins. Spar cap cross-sectional area, 0.41–0.24 in.^{2} (interior spars) and 1.6–0.92 in.^{2} (front and rear spars). Spar stiffener cross-sectional area, 0.006 in.^{2} (not designed). (All values decreasing from root to tip.) Material = $E = 1.0 \times 10^7$ lb/in.^{2}, $\nu = 0.33$, $\rho = 0.1$ lb/in.^{3} Allowable stresses: 60×10^3 lb/in.^{2} (tension and compression), 40×10^3 lb/in.^{2} (shear).

In Ref. 7, the sizes and locations of the structural elements of the 10-spar, 4-rib coarse model were selected and used as a nominal structural model. The structural mass of this wing was 497 lb. Additionally, concentrated weights were placed at the structural nodal points to simulate nonmodeled structural and nonstructural masses representing fuel, actuators, and stores. The aerodynamic model for the nominal and optimized structure consisted of 36 aerodynamic boxes with six chordwise and six spanwise divisions.

The 20-spar, 18-rib complex model was extensively modified from an original model by Love[8] for comparison to the coarse model. The wing box thickness profile was made identical to that of the coarse model. Each type of element was sized to obtain the same mass as in the coarse design, e.g., the total mass of the ribs in the complex model was equal to the total mass of the ribs in the coarse model, etc. Within this limitation, the thicknesses of the members were tapered from root to tip, as with the coarse model. The limited precision of the results from the ASTROS weight generator, which was used to find the weight of each structural group, and the leading-edge cutout on the complex model caused the final structural mass of the complex wing to be slightly lower than that of the coarse wing at 488 lb. A total load of 10,000 lb was first applied to each model at the tip nodes. The deflections of the two wings were within 5% of each other, as shown in Fig. 4. Then, a tip moment was applied in the form of opposite loads at the leading and trailing edges of the tip; this load case resulted in similar twists, also shown in Fig. 4. Finally, non-

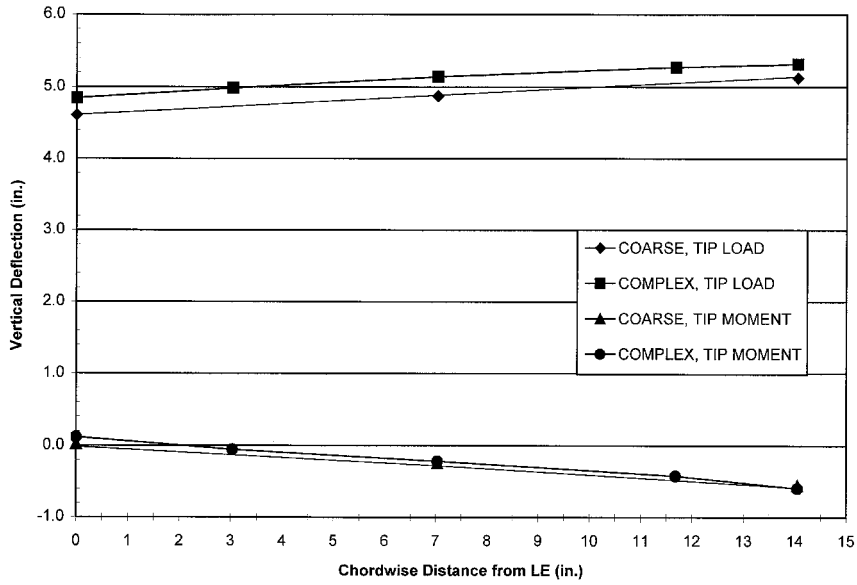

Fig. 4 Deflections because of tip loads and moments.

Table 1 Comparison of wing dynamic properties

Mode	Coarse frequency, Hz	Complex frequency, Hz
1	9.384	9.566
2	31.00	31.50
3	38.20	41.91
4	59.06	62.37

structural masses with a total mass equal to that on the coarse wing were placed in a straightforward pattern on the more complex wing and modified slightly so that the first few natural frequencies for the two models were within 10% of each other. Although the placement of these masses was not optimized to produce identical results, both mass distributions were reasonable first-cut placements for their respective models that have the same total mass. (See Table 1.)

Wing Structural Analysis

Before optimization, the nominal wing models were analyzed. ASTROS was used to determine the stresses in all structural elements resulting from a 9-*g* pull-up at sea level at M = 0.85. Additionally, the flutter speeds were determined for both models, together with the roll effectiveness at a dynamic pressure near the control reversal dynamic pressure.

These analyses were initially conducted in the subsonic regime (M = 0.85) using the USSAERO panel code for the steady flow and double-lattice aerodynamics for the unsteady flow as incorporated in ASTROS. It is noted that aerospace industry users of ASTROS have largely chosen to replace the built-in steady aerodynamic codes in Version 11 with their own in-house programs to achieve more accurate results.[9] The application of these subsonic aerodynamic theories resulted in the prediction of supersonic critical aeroelastic velocities: For the nominal coarse model a flutter speed of approximately 30,100 in./s (corresponding to a Mach number of M = 2.25 at sea level) was found for an input Mach number of M = 0.85 with a reversal dynamic pressure of approximately 45 psi (M = 2.09 at sea level). The optimized weights for M = 0.85 are reported here because they give insight into the sensitivity of the final weight on a specific constraint, even though the analysis is not physically meaningful. To provide more meaningful results, USSAERO for the steady flow and one of the supersonic aerodynamic formulations in ASTROS, the constant pressure method, were utilized in the continuation of this study. A Mach number of M = 1.2 was selected. When the coarse nominal model was analyzed at this supersonic Mach number, a slightly lower flutter speed of 29,600 in./s (M = 2.21) and a slightly lower reversal pressure of 41 psi (M = 2.00) were found.

Results for the nominal complex wing model differed slightly, but agreed within expected ranges given that the two wing models had similar first bending and torsion modes. For a Mach number of 0.85, the flutter speed of 32,300 in./s was only 7.3% higher than that for the coarse wing model.

However, the roll-reversal dynamic pressure, 31 psi (M = 1.73), for the complex model was considerably lower than for the coarse model. Because control reversal is caused by a quasi-static torque as a result of an increased pitching moment when a control surface is deflected, this result is surprising because the two wings have similar torsion characteristics. The variation of aileron effectiveness with dynamic pressure for this model is shown in Fig. 7.

When the nominal complex model was reanalyzed at M = 1.2, two effects were observed: first, the reversal pressure decreased to 21 psi, or M = 1.43 (Fig. 7). This indicates that, unlike for the coarse wing, the pressure obtained using subsonic analysis seems to be more in error, because it was 50% higher than that obtained using supersonic analysis. Second, the flutter speed actually increased to 38,100 in./s for the supersonic analysis. This does not necessarily represent an increase in the actual flutter speed of the wing; rather, it seems to be an effect of the method used to calculate the aerodynamic matrices for the flutter model. Whether the flutter speed goes down or up when the formulation is changed from subsonic to supersonic cannot be predicted in advance of running the analysis. To determine the actual flutter speed of the wing a matched-point iteration would need to be conducted.

Wing Structural Optimization

Coarse Wing

The coarse fighter wing structural model was optimized through resizing using ASTROS with both single and multiple constraints active at any given time (Table 2, Figs. 5 and 6). Some of these optimizations were originally performed in Ref. 7, but lower design variable minima were obtained here for the strength optimization. Because the strength-optimized sizes were used as side constraints for all subsequent optimizations, the change in these minima caused all subsequent flutter and aileron reversal results to differ slightly from those in Ref. 7. Five design variables were used: one each for the ribs, spar

Table 2 Weight optimized coarse wing model with various constraints

Model	Flight condition	Reversal-q, lb/in.^{2}	Flutter speed, in./s	Structural weight, lb
1. Nominal	M = 0.85	45	30,100	497
	M = 1.2	41	29,600	497
2. Optimized (strength)	M = 0.85	11	17,900	102
	M = 1.2	11	30,400	102
3. Optimized	M = 0.85	52[a]	32,100	405
	M = 1.2	52[a]	27,304	381
4. Optimized	M = 0.85	45[a]	29,500	398
	M = 1.2	41[a]	25,600	323
5. Optimized	M = 0.85	51	32,500[a]	440
	M = 1.2	57	32,500[a]	496
6. Optimized	M = 0.85	45[a] [55]	33,000[a]	424
	M = 1.2	41[a] [57]	33,000[a]	496
7. Optimized	M = 0.85	52[a]	31,000[a] [32,100]	405
	M = 1.2	52[a]	31,000[a] [32,900]	460

Note: Quantities in brackets denote the actual performance value in cases where the constraint was not active.
[a]Indicates quantity was a constraint.

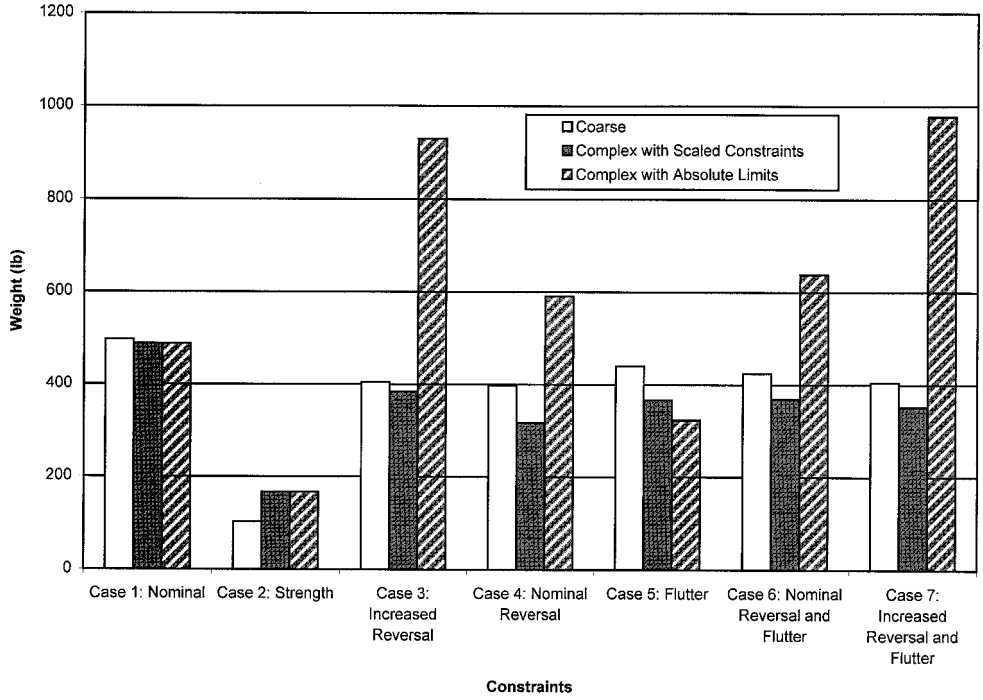

Fig. 5 Weight trends for subsonic cases.

webs, spar caps, quadrilateral skins, and triangular skins. The initial optimal structural model was obtained for a 9-g symmetric pull-up maneuver at M = 0.85 with a von Mises stress constraint and prescribed stress yield values applied to every structural element. The resulting structure weighed 102 lb, had a flutter speed of 17,900 in./s, and a roll reversal pressure of 11 psi. The following optimization studies were then conducted using these minimum allowable sizes as lower-size side constraints for all individual structural members.

Case 3 for the coarse structural model demonstrated that the nominal structure was not optimal for roll reversal. This model was optimized using an improved constraint for the reversal dynamic pressure of 52 psi with the same input Mach number of 0.85. This increase in the reversal dynamic pressure was accomplished while the structural weight of the optimized wing was reduced from a nominal weight of 497 to 405 lb. As a by-product, the flutter speed increased from 30,100 to 32,100 in./s.

Alternatively, when optimized for a less aggressive roll-reversal constraint of 45 psi (the value for the nominal model), the optimum weight was 398 lb; however, this structure had a lower flutter velocity (29,500 in./s) than the nominal model.

Two inconsistencies in the trends for the coarse wing are noted: Subsonic case 5 included only a flutter constraint only, whereas subsonic case 6 included a higher flutter speed constraint and a roll-reversal pressure constraint. Yet, the final-weight for case 6 was less than that for case 5. Obviously, the design ASTROS produced for case 5 was not a global optimum. The improvement in case 6 illustrates that adding constraints, even though they may not be active in the final design, can change the course of the optimization. It also reinforces the fact that numerical optimization schemes can only find local optima. The user must check these results, e.g., by using different initial conditions. The fact that case 5 was a local optimum was verified by the failure of the optimizer to find a feasible direction when the maximum allowable step size was reduced to a very small number. The only directions attempted violated the active flutter constraint.

Similarly, the results from supersonic cases 5 and 7 are inconsistent. Case 7 used a lower flutter speed constraint than

Table 3 Weight optimized complex wing model with various constraints

Model	Flight condition	Reversal-q, lb/in.^{2}	Flutter speed, in./s	Structural weight, lb
1. Nominal	M = 0.85	31	32,300	488
	M = 1.2	21	38,100	488
2. Optimized (strength)	M = 0.85	15	20,900	167
	M = 1.2	12	25,400	167
3. Optimized	M = 0.85	36[a]	45,200	384
	M = 1.2	36[a]	76,600	1690
	M = 0.85	52[a]	52,200	930
4. Optimized	M = 0.85	31[a]	52,600	317
	M = 1.2	21[a]	48,300	292
	M = 0.85	45[a]	46,700	591
5. Optimized	M = 0.85	35	34,900[a]	367
	M = 1.2	24	38,100[a]	372
	M = 0.85	32	32,500[a]	323
	M = 1.2	14	32,500[a]	305
6. Optimized	M = 0.85	31[a] [34]	35,400[a]	369
	M = 1.2	21[a]	35,400[a] [36,800]	292
	M = 0.85	45[a]	33,000[a] [43,400]	638
7. Optimized	M = 0.85	36[a]	33,300[a] [46,500]	352
	M = 1.2	36[a]	33,300[a] [b]	292
	M = 0.85	52[a]	31,000[a] [53,800]	978

Note: Quantities in brackets denote the actual performance value in cases where the constraint was not active.
[a]Indicated quantity was a constraint.
[b]All flutter roots were stable.

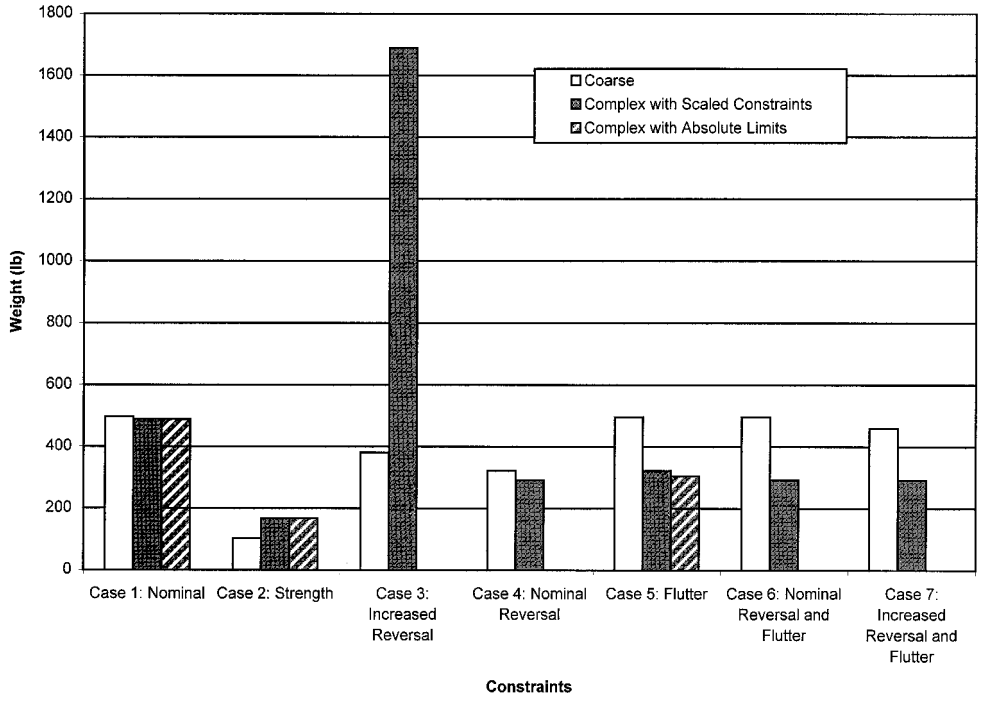

Fig. 6 Weight trends for supersonic cases.

case 5, along with a roll-reversal pressure constraint. The roll-reversal constraint drove the final design in case 7; the final flutter speed was higher than the constraint and higher than the constraint in case 5, yet the final weight in case 7 was lower.

Complex Wing

To provide a good comparison, the complex wing was optimized with the same types of constraints as the coarse wing. All results are presented in Table 3 and Figs. 5 and 6. First of all, because the nominal performances of the wings were different, equivalent constraints were developed based on the percentage increases that had been applied to the coarse wing. Alternatively, the constraints from the coarse wing were applied directly to the complex wing. Both of these methods were used here.

When optimized for a 9-g pull-up at M = 0.85, the optimal complex wing weighed 167 vs 102 lb for the coarse wing. The same number of design variables and the same linking scheme were used for both cases. The weight difference is a result of the larger element sizes in the coarse model, which tend to smear stresses and do not capture localized concentrations. The complex model, which does capture such concentrations, required some thicker elements to keep the stresses below material limits. The slightly heavier structure also caused the flutter speed to be slightly higher (20,900 vs 17,900 in./s). The roll reversal pressure for this case was 15 psi.

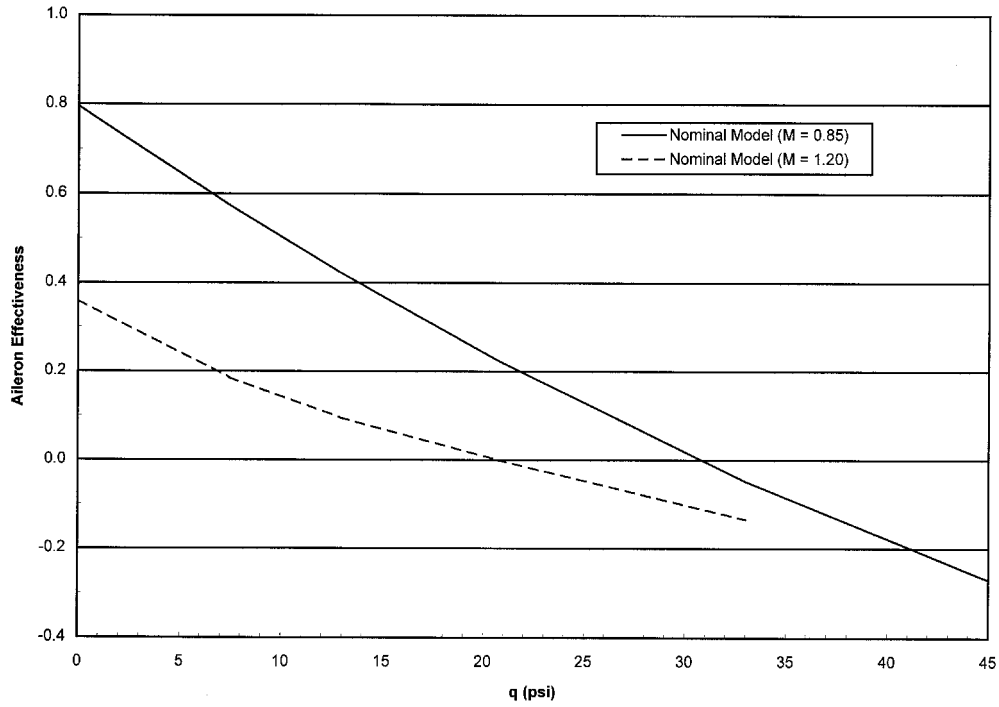

Fig. 7 Aileron effectiveness vs dynamic pressure, nominal complex wing.

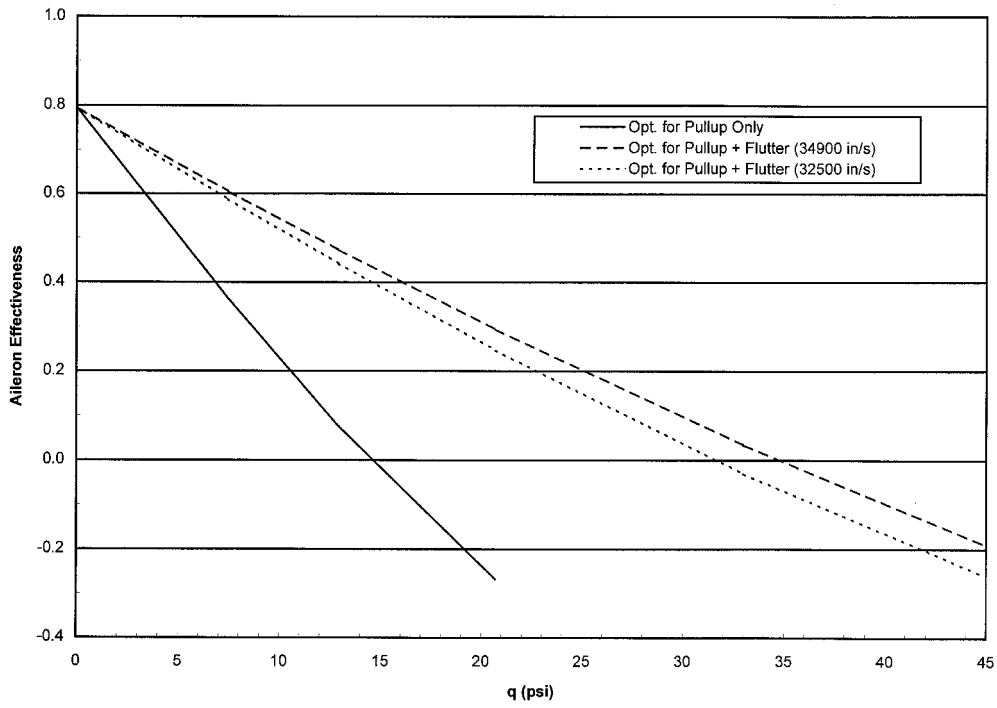

Fig. 8 Aileron effectiveness vs dynamic pressure, subsonic flutter optimization, complex wing model.

As with the coarse model, there are some inconsistencies in the results for the complex model. Cases 3 and 7 for $M = 0.85$ used a reversal pressure constraint of 36 psi. Case 7 also imposed a flutter speed constraint. The final design for case 7 had a higher flutter speed than that for case 3, yet it was lighter. Similarly, for $M = 1.20$, the case 7 design had the same reversal pressure as the case 3 design, but it was lighter. For case 3, the final design was very stiff and, thus, had a very high flutter speed, even though no flutter constraint was imposed. Finally, for cases 4 and 6 with absolute reversal constraints of 45 psi at $M = 0.85$, case 4 had a higher flutter speed, yet weighed less.

As with the coarse model each of these optima was verified as a local optimum by ensuring that no small design move could be made without violating a constraint.

During the optimizations that included control effectiveness constraints, ASTROS had difficulty converging to the optimum. It often oscillated between a feasible and an infeasible design on successive iterations rather than converging smoothly. Such oscillations seem to be caused by ill-conditioning of the roll-reversal constraint when the desired aileron effectiveness was close to zero; when constraints were other than zero, ASTROS quickly converged to an optimum. To minimize this effect, the design variable move limits were

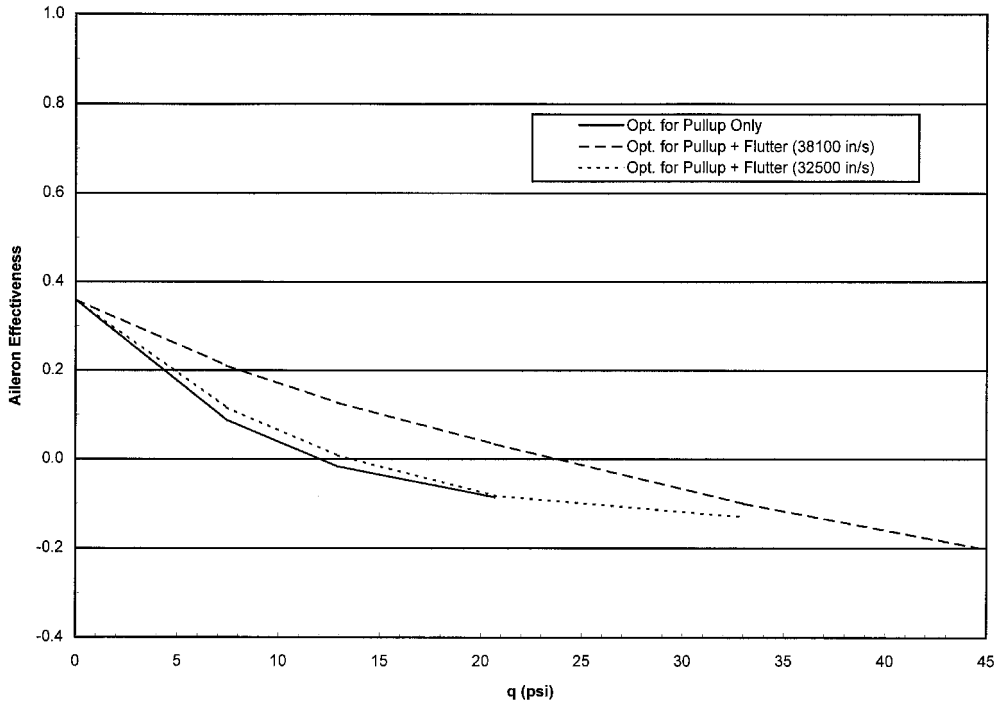

Fig. 9 Aileron effectiveness vs dynamic pressure, supersonic flutter optimization, complex wing model.

manually restricted and the constraint convergence criteria slightly relaxed.

ASTROS was unable to find designs for $M = 1.20$, when the same absolute roll-reversal constraints were applied as for the coarse wing. In each of these cases, it attempted unsuccessfully to satisfy the constraint by continually adding structural material; this increased the torsional stiffness, but not to the extent required to counteract the twisting moment at high dynamic pressures.

Conclusions

This effort examined the performance of ASTROS in optimizing two finite element models of a low-aspect ratio fighter-type wing. A range of constraints representative of the requirements for a modern combat aircraft were imposed, and the effects of these constraints on the final wing finite element weight was assessed. In general, ASTROS was able to increase the performance of the wing in one area, e.g., flutter speed or aileron reversal pressure, while decreasing its weight; when multiple constraints were imposed, as would be expected for an actual design, the weight savings were less pronounced.

The large discrepancies between the roll-reversal pressures for the coarse and complex nominal models, which carried over into the optimized results, and the large differences between the subsonic and supersonic reversal pressures for the complex wing model cannot be easily explained; however, it is again noted that aerospace industry users of ASTROS have largely chosen to replace the built-in steady aerodynamic codes. In addition, new aerodynamic modules are presently being incorporated into ASTROS. Despite these stated difficulties, the examples presented in this investigation demonstrate that the optimization capabilities of the ASTROS procedure are quite suited for the conceptual and preliminary design environments. Any number of constraints on strength, control reversal, and flutter can be imposed on general finite element structural models of flight vehicles. This ability to simultaneously consider many constraints from each of several disciplines allows the structural designer to develop nonintuitive solutions to the complex design problems representing modern flight vehicle structures.

References

[1]Neill, D. J., and Herendeen, D. L., "ASTROS Enhancements, Volume I—ASTROS User's Manual," Flight Dynamics Directorate, Wright Lab., TR-93-3025, Wright–Patterson AFB, OH, March 1993.

[2]Johnson, E. H., and Venkayya, V. B., "Automated Structural Optimization System (ASTROS), Volume I—Theoretical Manual," Air Force Wright Aeronautical Labs., TR-88-3028/I, Wright–Patterson AFB, OH, Dec. 1988.

[3]Neill, D. J., Johnson, E. H., and Herendeen, D. L., "Automated Structural Optimization System (ASTROS), Volume II—User's Manual," Air Force Wright Aeronautical Labs., TR-88-3028/III, Wright–Patterson AFB, OH, Dec. 1988.

[4]Yurkovich, R., "The Use of Taguchi Techniques with the ASTROS Code for Optimum Wing Structural Design," *Proceedings of the AIAA/ASME/ASCE/AHS/ASC 35th Structures, Structural Dynamics, and Materials Conference*, AIAA, Washington, DC, 1994, pp. 1334–1342.

[5]Striz, A. G., and Venkayya, V. B., "Influence of Structural and Aerodynamic Modeling on Flutter Analysis," *Journal of Aircraft*, Vol. 31, No. 5, 1994, pp. 1205–1211.

[6]Striz, A. G., and Venkayya, V. B., "Influence of Structural and Aerodynamic Modeling on Optimization with Flutter Constraint," *Proceedings of the 3rd USAF/NASA Symposium on Recent Advances in Multidisciplinary Analysis and Optimization* (San Francisco, CA), U.S. Air Force Wright Research and Development Center, Wright–Patterson AFB, OH, 1990.

[7]Striz, A. G., Eastep, F. E., and Venkayya, V. B., "Influence of Static and Dynamic Aeroelastic Constraints on the Optimal Structural Design of Flight Vehicle Structures," *Proceedings of the AIAA/ASME/ASCE/AHS/ASC 32nd Structures, Structural Dynamics, and Materials Conference*, AIAA, Washington, DC, 1991, pp. 470–476.

[8]Love, M. H., Barker, D. K., and Bohlmann, J. D., "An Aircraft Design Application Using ASTROS," Flight Dynamics Directorate, Wright Lab., WL-TR-93-3037, Wright–Patterson AFB, OH, June 1993.

[9]Chen, P. C., Sarhaddi, D., Liu, D. D., Karpel, M., Striz, A. G., and Jung, S. Y., "A Unified Unsteady Aerodynamic Module for Aeroelastic, Aeroservoelastic and MDO Applications," *Proceedings of the Confederation of European Aerospace Societies International Forum on Aeroelasticity and Structural Dynamics* (Rome, Italy), Confederation of European Aerospace Societies, Rome, Italy, 1997, pp. 123–139.